Femtosecond IR Study of Excited-State Relaxation and Electron-Injection Dynamics of $Ru(dcbpy)_2(NCS)_2$ in Solution and on Nanocrystalline TiO_2 and Al_2O_3 Thin Films

John B. Asbury,[†] Randy J. Ellingson,[‡] Hirendra N. Ghosh,[†] Suzanne Ferrere,[‡] Arthur J. Nozik,*[,‡] and Tianquan Lian*[,†]

Department of Chemistry, Emory University, Atlanta, Georgia 30322, and National Renewable Energy Laboratory, 1617 Cole Boulevard, Golden, Colorado 80401

Received: September 30, 1998; In Final Form: February 10, 1999

The photophysics and electron injection dynamics of $Ru(dcbpy)_2(NCS)_2$ [dcbpy = (4,4′-dicarboxy-2,2′-bipyridine)] (or Ru N3) in solution and adsorbed on nanocrystalline Al_2O_3 and TiO_2 thin films were studied by femtosecond mid-IR spectroscopy. For Ru N3 in ethanol after 400 nm excitation, the long-lived metal-to-ligand charge transfer (^{3}MLCT) excited state with CN stretching bands at 2040 cm^{-1} was formed in less than 100 fs. No further decay of the excited-state absorption was observed within 1 ns consistent with the previously known 59 ns lifetime. For Ru N3 absorbed on Al_2O_3, an insulating substrate, the ^{3}MLCT state was also formed in less than 100 fs. In contrast to Ru N3 in ethanol, this excited state decayed by 50% within 1 ns via multiple exponential decay while no ground-state recovery was observed. This decay is attributed to electron transfer to surface states in the band gap of Al_2O_3 nanoparticles. For Ru N3 adsorbed onto the surface of TiO_2, the transient mid-IR signal was dominated by the IR absorption of injected electrons in TiO_2 in the 1700−2400 cm^{-1} region. The rise time of the IR signal can be fitted by biexponential rise functions: 50 ± 25 fs (>84%) and 1.7 ± 0.5 ps (<16%) after deconvolution of instrument response function determined in a thin silicon wafer. Because of the scattering of the pump photon in the porous TiO_2 thin film, the instrument response may be slightly lengthened, which may require a faster rise time for the first component to fit the data. The first component is assigned to the electron injection from the Ru N3 excited state to TiO_2. The amplitude of the slower component appears to vary with samples ranging from ca. 16% in new samples to <5% in aged samples. The subsequent dynamics of the injected electrons have also been monitored by the decay of the IR signal. The observed 20% decay in amplitude within 1 ns was attributed to electron trapping dynamics in the thin films.

1. Introduction

Photoelectrochemical solar cells based on dye-sensitized TiO_2 films have received much attention in recent years because of their potential applications as a cost-effective alternative to silicon-based cells.[1−5] Since the report by Graetzel's group that solar cells based on $Ru(dcbpy)_2(NCS)_2$ [dcbpy = (4,4′-dicarboxy-2,2′-bipyridine)] (or Ru N3)-sensitized nanocrystalline TiO_2 thin films can achieve a solar to electric power conversion efficiency of about 10%,[6,7] electron injection and recombination properties of Ru-dye-sensitized semiconductors have been studied by many groups.[8−24] Although different studies have reported very different time scales of electron injection, it is generally agreed that the high-energy conversion efficiency can be attributed to fast-electron injection from the sensitizer to the semiconductor and much slower back electron transfer (ET) to the sensitizer.[3]

The exact nature and time scale of the electron injection step for Ru N3 have been subjects of a recent debate.[12,14] Electron injection in Ru N3-sensitized nanocrystalline TiO_2 films in an ethylene carbonate/propylene carbonate (1:1) solution was reported originally to be a biphasic process with time constants of <150 fs and 1.2 ps in a visible transient absorption study. A more recent study by Hanappel et al.[12] reported different transient spectra for samples in ultrahigh vacuum (UHV). The exact assignment of these different electronic spectra is still a subject of current debate.[25,26] The difficulty of assigning the complex transient spectra of dye molecules can be avoided by using a technique that can directly probe injected electrons. In the study by Hanappel et al.,[12] a transient near-IR signal at 1100 nm was observed and assigned to injected electrons in TiO_2. However, in a more recent study under atmospheric conditions that probed at 1500 nm, similar transient absorption signals for Ru N3 in ethanol and for Ru N3 on ZrO_2 were reported.[9] The rise time of the signal appears to be similar to the signal observed in Ru N3 on TiO_2 thin films under the same experimental condition, but the amplitude is somewhat smaller.[9] This study indicates that the transient near-IR signal may contain non-negligible contributions from the electronic transitions of the sensitizer in the Ru N3 dye-sensitized system under normal atmospheric conditions. This near-IR probe technique for studying electron transfer may face similar difficulty as earlier studies in the visible region: the possible spectral overlap of the ground state, excited singlet state, triplet state of the neutral sensitizer, the ground state of the cation, and the absorption of injected electrons.

Recently, transient mid-IR spectroscopy was used to study electron transfer in sensitized nanoparticles.[8−10,27,28] Unlike

* To whom correspondence should be addressed. E-mail: T.L., tlian@emory.edu; A.J.N., anozik@nrel.nrel.gov.
[†] Emory University.
[‡] National Renewable Energy Laboratory.

10.1021/jp983915x CCC: $18.00
Published on Web 03/26/1999

previous studies in the near-IR region, this technique can directly probe the mid-IR absorption of electrons inside semiconductors without the complication of broad electronic transitions of the adsorbates. It has been well-demonstrated that in bulk[29,30] and quantum well[31] semiconductor materials, conduction band electrons in semiconductors have strong absorptions in the infrared region. These absorptions consist of free carrier absorption,[32] which is often broad and increases with wavelength, intraband transitions[32] between different valleys (or subbands) within the conduction band, and absorptions of trap states. Since the IR absorption of electrons is direct evidence for the arrival of electrons inside nanoparticles, it can be used as an unambiguous spectroscopic probe for studying interfacial electron transfer between a semiconductor and its adsorbates.

We have recently studied electron-transfer dynamics in Ru N3-sensitized TiO_2 thin films using femtosecond mid-IR spectroscopy. In an earlier Letter, we reported the ultrafast injection time for Ru N3-sensitized nanocrystalline TiO_2 thin film using femtosecond IR spectroscopy in the near- to mid-IR region.[9] The observed ultrafast electron injection from the Ru N3 excited state to TiO_2 in about 50 fs suggests that electron-injection dynamics can occur on the same time scale as intramolecular vibrational relaxation and intersystem crossing in these Ru dye molecules. In this paper, we will examine the excited-state dynamics of Ru N3 in solution and adsorbed on Al_2O_3 films. These dynamics will be compared with the electron-injection dynamics for Ru N3 on TiO_2 thin films. In addition, the dynamics of the injected electrons in TiO_2 films will also be discussed.

2. Experimental Section

Femtosecond IR Spectrometer. The femtosecond infrared spectrometer at Emory University used for this study is based on an amplified femtosecond Ti:sapphire laser system from Clark-MXR (1 kHz repetition rate at 800 nm, 100 fs, 900 μJ/pulse) and nonlinear frequency mixing techniques. The details of this set up have been described elsewhere.[27,28] Briefly, the 800 nm output pulse from the regenerative amplifier is split into two parts. One part, with about 600 μJ/pulse, is used to pump a Clark IR optical parametric amplifier to generate two tunable near-IR pulses from 1.1 to 2.5 μm. These signal and idler pulses are combined in an $AgGaS_2$ crystal to generate mid-IR pulses from 3 to 10 μm by difference frequency generation. The mid-IR pulses have a typical intensity fluctuation of 1−3%. The remaining part of the 800 nm pulse, with 300 μJ/pulse, is frequency doubled in a BBO crystal to generate pump pulses at 400 nm. The probe IR pulses are divided into a signal beam and a reference beam. While the signal beam measures the absorption of the sample, the reference beam is used to normalize the laser intensity fluctuation. Both beams are then dispersed in a monochromator. A 2−3 cm^{-1} slice of the total spectrum (approximately 200 cm^{-1}) is measured by a pair of MCT detectors for each laser pulse. To minimize low-frequency laser fluctuations, the main noise source, every other pump pulse is blocked with a synchronized chopper (New Focus model 3500) at 500 Hz, and the absorbance change is calculated with two adjacent probe pulses (pump blocked vs pump unblocked). Transient absorption spectra are recorded by scanning the monochromator at a fixed pump probe delay time. Kinetics data are taken at fixed wavelength while scanning the delay time.

In all the experiments presented here, a flowing solution sample or a moving film sample was pumped at 400 nm and the subsequent absorbance change in the 1950−2200 cm^{-1} region was measured. The pump energy varies from 1 to 10 μJ depending on the sample, as indicated below. The diameters of the pump and probe beams at the sample were 500 and 300 μm, respectively. The instrument response for a 400 nm pump mid-IR probe experiments was determined in a thin silicon wafer, in which the absorption of 400 nm photons led to instantaneous generation of free carriers that absorbed strongly in the mid-IR region. The typical instrument response function measured was well-presented by a Gaussian function with a full width at half-maximum (fwhm) of about 190 fs.

Sample Preparations. TiO_2 nanoparticle colloids were prepared as previously described, using Degussa P25 TiO_2 (about 70% anatase and 30% rutile) as starting material.[6] The Al_2O_3 nanoparticle colloid was prepared using a method similar to that used for TiO_2. The starting materials were Degussa Aluminum Oxide C (primary particle size of 13 nm). Some adjustment of the ratio of starting material weight to distilled water volume was required for the Al_2O_3 preparation. Thin films were prepared using these colloids as previously described.[9] The films were prepared on c-cut polished sapphire substrates and fired at 450 °C for 45 min in air. TiO_2 and ZrO_2 films were 5 μm thick with good transparency. The Al_2O_3 films were ∼15 μm thick and showed greater scattering than the TiO_2 films. Immersion and storage of the TiO_2 and Al_2O_3 films in a room temperature ethanol solution containing 200 μM Ru N3 and 20 mM chenodeoxycholic acid resulted in adsorption of the Ru N3 to the porous film surface. The resulting dye-sensitized films showed an absorbance of ∼1.0 at 400 and 550 nm. The absorbance at 400 nm for a typical naked film used in the experiment was about 0.3 OD with contributions from both absorption and scattering of the nanocrystalline films. High-purity Ru N3 was purchased from Solaronix (Lausanne, Switzerland).

3. Results

Ru N3 in Ethanol. To understand the detailed electron-injection dynamics of the Ru N3-sensitized TiO_2 films, the excited-state dynamics of the sensitizer molecules themselves, without the complication of electron injection, need to be understood. We have studied the excited-state dynamics of Ru N3 (1) in ethanol solution and (2) adsorbed on Al_2O_3 film, a large band gap substrate.

Shown in Figure 1b are transient IR spectra in the CN stretching mode region of Ru N3 in ethanol (connected full circles) and adsorbed in Al_2O_3 film (connected open circles) at 5 ps after 400 nm excitation. Shown in Figure 1a are ground-state FT-IR spectra of the dye in ethanol (solid line) and adsorbed on Al_2O_3 film (dotted line). The excitation leads to bleach of the ground-state absorption at 2115 cm^{-1} and a small shoulder at 2140 cm^{-1}, while creating two new bands at 2040 and 2075 cm^{-1}. Shown in Figure 2 are transient kinetics of the sensitizer in solution measured at the peaks of the transient spectrum: (a) 2115, (b) 2075, and (c) 2040 cm^{-1}. The kinetics at longer time at (a) 2115 and (b) 2040 cm^{-1} are shown in Figure 3. The full circles in these figures are the experimental data, and the solid lines are obtained fits by convolution of a single-exponential rise function with the instrument response function. For the kinetics trace at 2040 cm^{-1} (Figure 2c), the rise time of the signal appears to be instrument response time limited. An instrument response time limited rise measured in a thin silicon wafer, as indicated by the dashed curve, and a fit with a 75 fs single-exponential rise time (solid curve) are shown for comparison. Within the signal-to-noise ratio of the data, satisfactory fits can be obtained for single-exponential rise time constant of $<$75 fs, which is considered as the upper limit of the rise time.

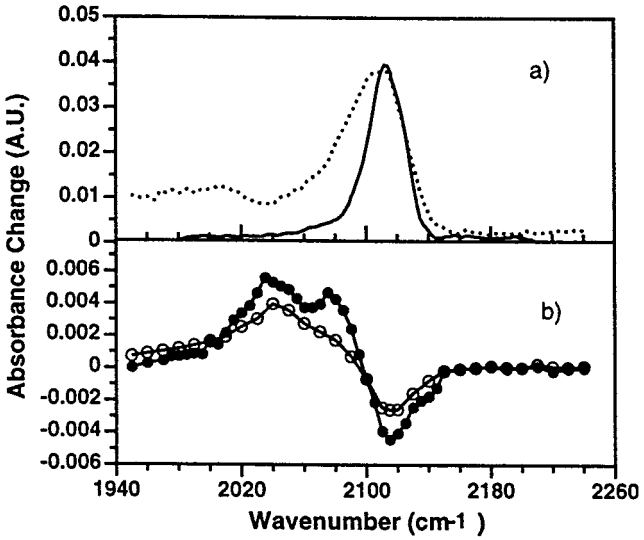

Figure 1. (a) Ground-state FTIR spectra of Ru N3 in ethanol (solid line) and on Al_2O_3 film (dotted line). (b) Transient IR difference spectra of Ru N3 in ethanol (full circles) and on Al_2O_3 film (open circles) at 5 ps after 400 nm excitation.

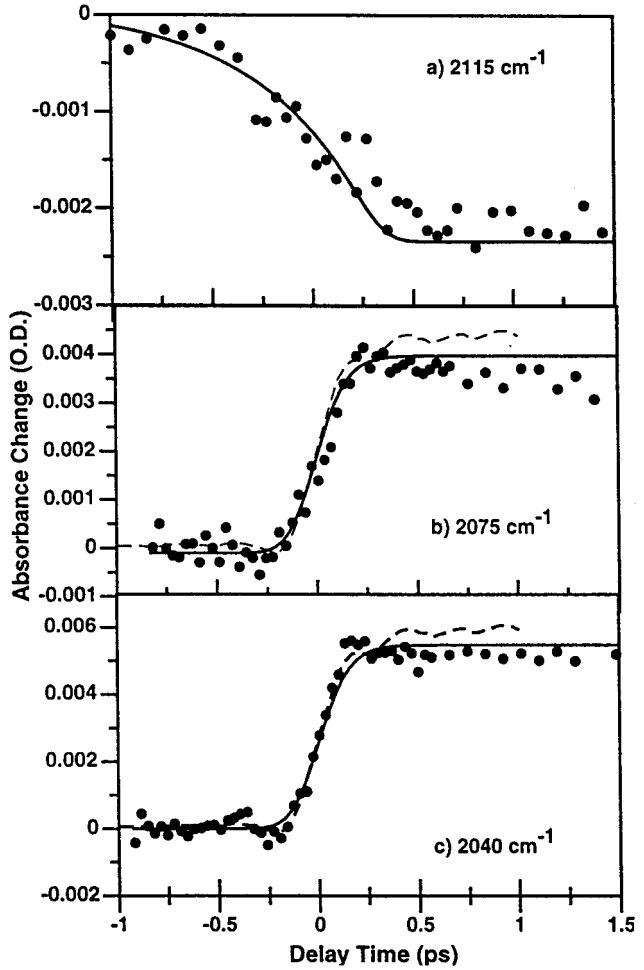

Figure 2. Transient kinetics of Ru N3 in ethanol measured at the peaks of the transient spectrum: (a) at 2115, (b) at 2075, and (c) at 2040 cm^{-1}. Filled circles are data points, solid lines are best fits, and dashed lines indicate the instrument response measured in silicon. The fits in (b) and (c) are single-exponential rise with a 75 fs time constant, and the fit in (a) includes PFID (see main text).

For the kinetics trace at 2075 cm^{-1} (Figure 2b), reasonable fits can be obtained with a rise time of 75 ± 50 fs. The formation

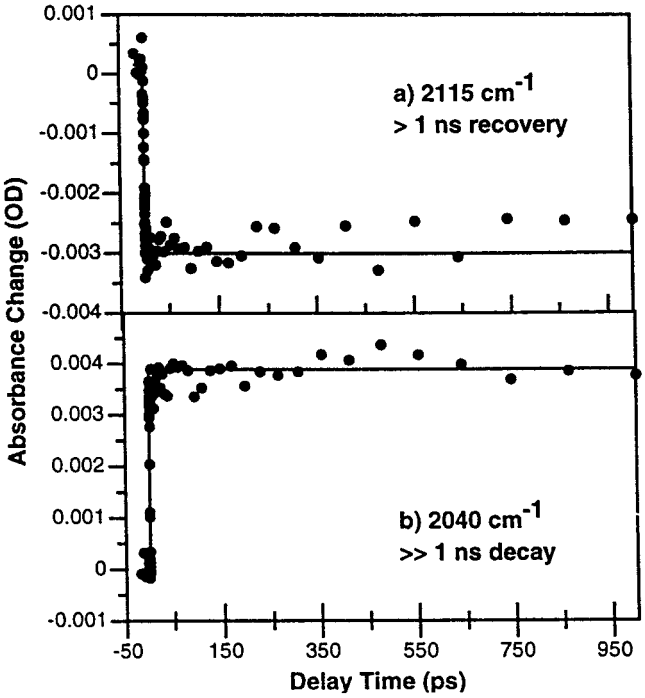

Figure 3. Kinetic traces of Ru N3 in ethanol taken at the two main peaks of the transient spectrum, (a) 2115 and (b) 2040 cm^{-1}. The filled circles are the data and the solid lines are the fits.

of the bleach at 2115 cm^{-1} appears to be slower as shown in Figure 2a. This slow rise can be attributed to perturbed free induction decay.[33] The absorbance change at these peak wavelengths shows negligible decay in the nanosecond time scale, as shown in Figure 3. Satisfactory fits of the data can be obtained with decay functions with time constants ≫1 ns.

Ru N3 on Al_2O_3. Since electron injection occurs from adsorbed Ru N3 molecules on the TiO_2 surface, it is more relevant to study the excited-state dynamics of adsorbed dye molecules on a noninjecting substrate. The band gap for Al_2O_3 is about 8 eV,[47] and its conduction band is not accessible by the excited state of the dye.[22]

The transient spectrum of Ru N3 adsorbed on Al_2O_3 is shown by the connected open circles in Figure 1b. A 400 nm excitation leads to a bleach of the peak at 2115 cm^{-1} for adsorbed Ru N3 and the generation of a new band at 2040 cm^{-1}. Shown in Figure 4 is a transient kinetics scan of Ru N3 adsorbed on Al_2O_3 film measured at 2040 cm^{-1}. Because of the poor data quality and small number of data points on the rising edge of the data, the rise time of the signal cannot be determined accurately. Shown by the solid and dash curve are fits with single-exponential rise time of 1 fs (to represent no rise time) and 100 fs. Within the signal-to-noise, satisfactory fits to the data can be obtained with single-exponential rise times of <100 fs. The kinetics on a longer time scale are shown in Figure 5 for probe wavelength at (a) 2115 and (b) 2040 cm^{-1}. The best fit to the data at 2115 cm^{-1}, represented by the solid line in Figure 5a, shows again a >1 ns recovery, similar to the bleach recovery kinetics for Ru N3 in ethanol. The transient absorption at 2040 cm^{-1} for Ru N3 on Al_2O_3 decays by about 50% by 1 ns, very different from that of Ru N3 in ethanol. The decay kinetics can be fit by a biexponential decay function plus a long-lived component with the following time constants and initial amplitudes (in parentheses): 3.5 ps (21%), 130 ps (26%), and ≫1 ns (53%), as shown by the solid line in Figure 5b. The dashed line, shown in Figure 5b for comparison, indicates a ≫1 ns decay component similar to that observed for Ru N3 in ethanol.

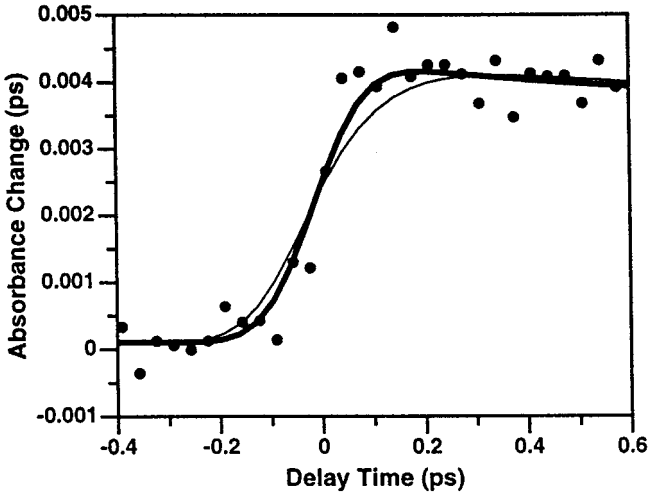

Figure 4. Transient kinetics of Ru N3-sensitized Al_2O_3 film taken at 2040 cm^{-1}. The data are filled circles. A 1 fs fit (heavy line), representing negligible rise time, and a 100 fs fit (light line) are shown.

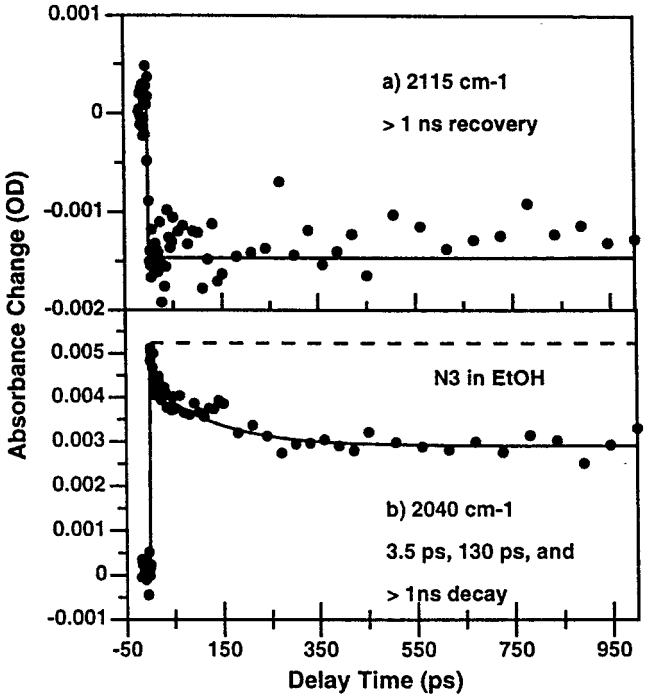

Figure 5. Kinetics traces of Ru N3-sensitized Al_2O_3 film measured at the peaks of the transient spectrum (data are filled circles): (a) at 2115 cm^{-1} with >1 ns recovery like Ru N3 in ethanol and (b) at 2040 cm^{-1} with a multiexponential fit (solid line) showing 3.5 ps, 130 ps, and >1 ns decay components in contrast to Ru N3 in ethanol (dashed line).

Ru N3 on TiO_2. Shown in Figure 6 is a comparison of transient IR signals in thin films of Ru N3-sensitized TiO_2, naked TiO_2, and Ru N3-sensitized Al_2O_3 measured at 2040 cm^{-1} with 1.1 μJ of 400 nm excitation. It should be pointed out that the data shown in Figures 1b, 4, and 5 for Ru N3-sensitized Al_2O_3 were collected with seven times higher pump power. At the reduced pump power, the transient IR signals for Ru N3-sensitized Al_2O_3 film is negligible, as indicated by the dotted curve. The signal in the naked TiO_2 film is about 0.6 OD, about 10 times smaller than that in Ru N3-sensitized TiO_2 thin films. We found that the signal in Ru N3-sensitized TiO_2 thin films was very broad and can be observed in the 1700−2400 cm^{-1} region. This signal is assigned to injected electrons in TiO_2 (see below).

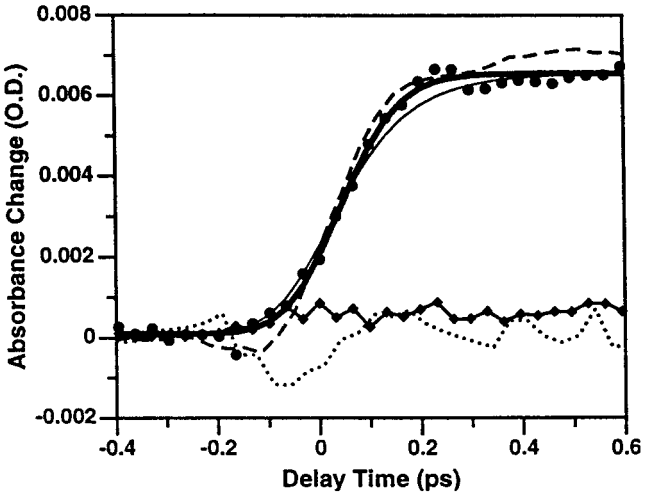

Figure 6. Comparison of signals in films of Ru N3-sensitized TiO_2 (filled circles), naked TiO_2 (connected diamonds), and Ru N3-sensitized Al_2O_3 (dotted line) probed at 2040 cm^{-1} after 400 nm excitation. A 50 fs fit (heavy line) and a 100 fs fit (light line) are shown with the instrument response taken in silicon for comparison (dashed line).

The rise time of the data shown in Figure 6 for Ru N3-sensitized TiO_2 thin films can be well fit by a single-exponential rise function convoluted with the instrument response function. The best fit to the data at 2040 cm^{-1} yielded a 50 fs rise as shown by the solid line. The fitting procedure allowed $t = 0$ to vary, which caused some uncertainty in the fitting of the rise time. This uncertainty is included in the error bar of ±25 fs, which reflects a 50% increase of the χ^2 of the fit. The light line in Figure 6 shows a similar curve with a 100 fs rise time, which cannot give a satisfactory fit to the data. A similar rise time has been observed at probe wavelengths in the 2000−2200 cm^{-1} region. Shown in Figure 7 are transient kinetics for Ru N3-sensitized TiO_2 at (a) 2083, (b) 2115, and (c) 2160 cm^{-1}. The full circles are experimental data, and the solid lines are the best fits to the data. The rise of the data at these three other wavelengths can be well fit by a single-exponential rise function convoluted with the instrument response function. The best fits to these data yielded rise time constants between 50 and 75 fs. At wavelengths with high-quality data, such as 2040, 2115, and 2160 cm^{-1}, the range of the rise time constants that could produce a good fit was determined to be about ±25 fs of the best fit. We, therefore, report an average rise time of 50 ± 25 fs. In addition to this fast injection component, there appears to be a much smaller and slower rise component in the picosecond time scale. Figure 8 shows the kinetics up to 10 ps for Ru N3-sensitized TiO_2 film probed at (a) 2040, (b) 2115, and (c) 2150 cm^{-1}. The kinetics can be well-fit by two exponential rise functions. The rise time of the fast component was fixed at 50 fs, which was determined by the short kinetics shown in Figures 6 and 7. Best fits to the data yield time constants for the second rise component of 1.7 ± 0.5 ps. The relative amplitudes for both components at each wavelength are listed in Table 1.

Shown in Figure 9 are decay kinetics of the transient IR signals measured in Ru N3-sensitized TiO_2 films (full circles) and naked TiO_2 films (open circles). The signals from the naked film were measured at seven times higher pump power compared to those of the sensitized film. The decay of the IR signals in the sensitized film can be fitted by double-exponential-decay functions and the decay in unsensitized film can be well-fit by three-exponential-decay functions. The best fits of the data using these models are listed in Table 1. The slowest decay

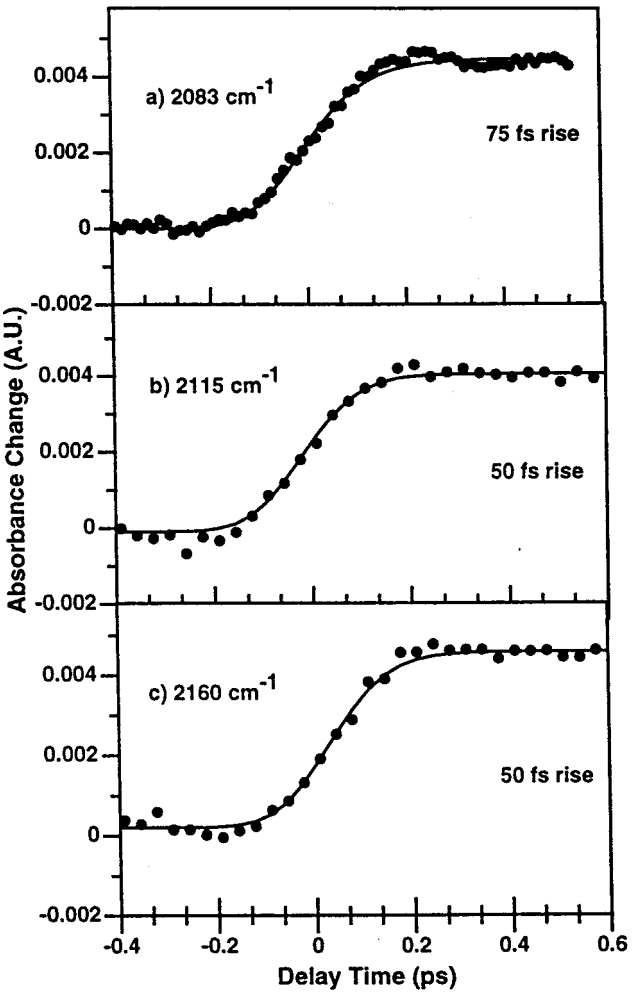

Figure 7. Transient kinetics of Ru N3-sensitized TiO_2 film at (a) 2083, (b) 2115, and (c) 2160 cm^{-1}. The data are full circles and fits are solid lines showing a 50−75 fs rise.

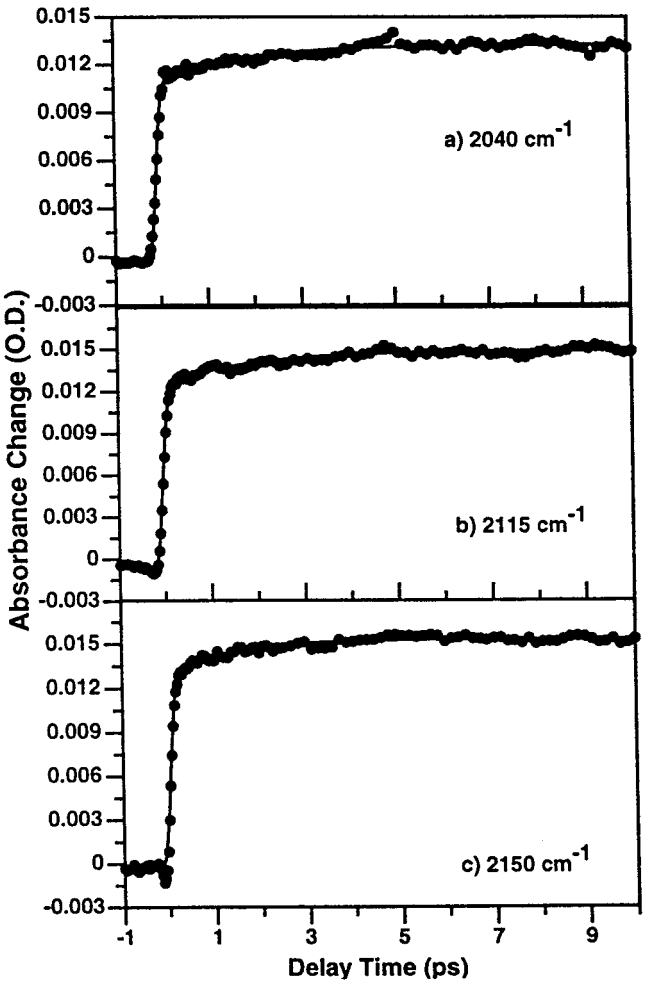

Figure 8. Transient kinetics of Ru N3-sensitized TiO_2 film at (a) 2040, (b) 2115, and (c) 2150 cm^{-1}. The data are full circles and the biexponential fits are solid lines showing a fast 50 fs rise and a slower 1.7 ± 0.5 ps rise.

component is larger than 1 ns and is not well-determined by our data because of the limited delay time.

4. Discussions

1. Photophysics of Ru N3 in Solution. As shown in Figure 1, excitation at 400 nm led to the bleach at 2115 cm^{-1} and the small shoulder at 2140 cm^{-1}. The bleach at 2115 cm^{-1} is identical to the peak of the CN stretching mode of freshly prepared Ru N3, as shown by the FTIR spectrum of Ru N3 in ethanol. This peak, with a fwhm of about 30 cm^{-1}, contains both the symmetric and asymmetric CN stretching modes. The small shoulder at 2140 cm^{-1} was not observed in the FTIR spectrum of freshly prepared Ru N3 in ethanol solution but could be seen in samples that were a few days old. This shoulder was also absent in the FTIR spectra of Ru N3-sensitized Al_2O_3 and TiO_2 thin films that were used in the experiments. The small shoulder present in the old solution samples may have resulted from protonation of the Ru N3 because of the increasing amount of water dissolved in ethanol from exposure to air. This could not occur for Ru N3 adsorbed on the films since the carboxylate groups were bound to the surface.

Two new CN stretching absorption bands in the excited state were observed at 5 ps after the excitation, as shown in Figure 1. These bands at 2040 and about 2075 cm^{-1} are shifted to lower energy compared to their respective ground-state CN stretching modes at 2115 and 2140 cm^{-1}. For Ru N3 in solution, its UV−vis spectrum shows two strong ^{1}MLCT bands centered at 395 and 530 nm. Excitation at 400 nm promotes an electron from the Ru(II) π symmetry d-orbitals to the dcbpy π^* orbital forming Ru(III). The SCN^- ligand can be represented as a superposition of the following two resonant structures:

$$\text{(a) Ru:N}\equiv\text{C}-\text{S:::}^{(-1)} \quad \text{(b) Ru::N}^{(-1)}=\text{C}=\text{S::}$$

In the ground state, structure a is more favorable. In the MLCT excited state, the Ru(III) metal center has a smaller electron charge density, which favors the more negatively charged N atom of the NCS ligand. So the excited state may have more character of structure b compared to the ground state, which leads to a weakened CN bond strength. This is consistent with the observed decrease of the CN stretching frequency in the excited state. In fact, a NCS^- group to Ru(III) charge-transfer band has been observed for the cationic form of the Ru(III) N3 in solution or on TiO_2,[14] supporting the explanation above.

In a previous study on $Ru(bpy)_3^{+2}$, it was found that the long-lived ^{3}MLCT in this Ru complex was formed on the sub-picosecond time scale.[34] We, thus, expect that the Ru N3 may also relax from the initially excited ^{1}MLCT state to its lowest lying excited state, ^{3}MLCT, in the sub-picosecond time scale. The observed spectrum at 5 ps is most likely that of the ^{3}MLCT state. The formation and decay time of the excited ^{3}MLCT state can be obtained from the kinetics measured at the three different

TABLE 1: Summary of Rise and Decay Kinetics Measured in Ru N3-Sensitized and Naked TiO_2 Films

wavenumbers	N_3/TiO_2 rise time short scan (−1 to 1 ps)	N_3/TiO_2 rise time medium scan (−1 to 10 ps)	N_3/TiO_2 decay time long scan (−10 ps to 1 ns)	naked TiO_2 decay time long scan (−10 ps to 1 ns)
2040	50 ± 25 fs	50 fs (83%) +1.9 ps (17%)	100 ps (22%) +5.6 ns (78%)	12 ps (22%) +200 ps (24%) +3 ns (54%)
2080	75 ± 25 fs			
2115	50 ± 25 fs	50 fs (86%) +1.9 ps (14%)	200 ps (15%) +8 ns (85%)	7 ps (22%) +150 ps (24%) +2.6 ns (54%)
2150		50 fs (84%) +1.3 ps (16%)	7 ns (100%)	15 ps (23%) +3.4 ns (77%)
2160	50 ± 25 fs			
average	50 ± 25 fs	50 fs (84%) +1.7 ± 0.5 ps (16%)		

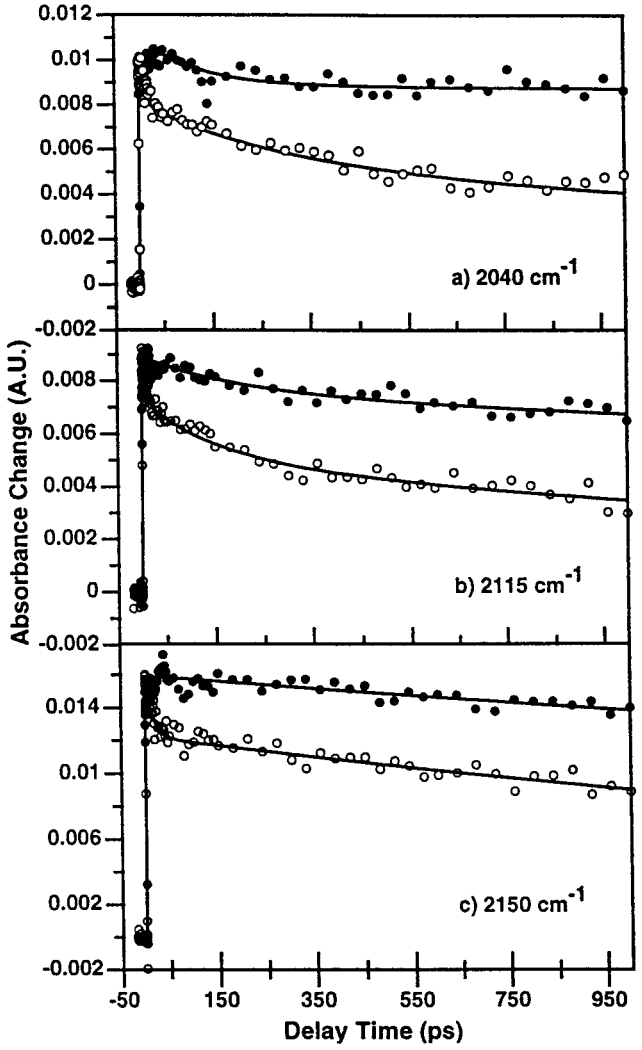

Figure 9. Decay kinetics of transient IR signals measured in Ru N3-sensitized TiO_2 film (full circles) and naked TiO_2 film (open circles). Solid lines are fits to the data showing multiexponential decay components for both sensitized and naked films.

peak positions for the ground and excited state, as shown in Figures 2 and 3. The appearance of the excited state was found to occur in less than 100 fs according to the best single-exponential fit of the data. These signals show no noticeable decay for delay times up to 1 ns. This result suggests that upon 400 nm excitation, the molecule relaxes to its lowest lying ^{3}MLCT state in less than 100 fs and stays there for over 1 ns. This result is consistent with the previous observation of an ultrafast formation time[34] and a 59 ns lifetime of the ^{3}MLCT state.[6] It should be pointed out that the above assignment of the ^{3}MLCT state formation time is based on the assumption that the CN stretching mode in the ^{3}MLCT state is different from that in the ^{1}MLCT state. To the best of our knowledge, we are not aware of any published results on the possible shift of CN stretching frequency in similar compounds. Since the charge distribution on the Ru(III) center may be different in these two excited states, the amount of charge transfer from NCS to Ru(III) and back-donation may be different. Therefore, it is not unreasonable to expect a noticeable shift (>5 cm^{-1}) in the CN stretch frequency upon relaxation from ^{1}MLCT to ^{3}MLCT state. However, if the CN stretch frequencies are similar in the ^{1}MLCT and ^{3}MLCT states, the measured <100 fs rise time does not indicate the ^{3}MLCT state formation time.

2. Photophysics of Ru N3 Adsorbed on Al_2O_3. Adsorption of Ru N3 on substrates results in only a slight shift and broadening of the CN stretch in the ground state.[35] The general features of the UV−vis spectrum are still the same as the spectrum in solution, showing two MLCT bands at 395 and 530 nm. The detailed shape and possible shift of the bands were not well-determined in our samples because of the scattering nature of the Al_2O_3 film in this region. A previous diffuse reflectance measurement of a similar Ru dye, $Ru(bpy)_2(dcbpy)^{2+}$, has found a slight extension of the lower MLCT band to the longer wavelength region upon adsorption on Al_2O_3 and TiO_2, indicating a charge-transfer interaction between the Ru dye and the substrates.[19] For Ru N3 on Al_2O_3, excitation at 400 nm is again expected to promote an electron from the Ru π symmetry d-orbitals to the dcbpy π^* orbitals, forming Ru(III). The general features of the transient IR spectrum, as shown in Figure 1, are still the same compared to that of Ru N3 in solution, except the absence of the small shoulder at 2140 cm^{-1} and the corresponding absorption band at about 2075 cm^{-1}. A similar spectral shift to lower energy in the excited state was observed and can be explained in a manner similar to that of Ru N3 in ethanol solution, as discussed in the earlier section.

The rise time of the transient absorption at 2040 cm^{-1} was also found to be <100 fs according to the best fit of kinetics shown in Figure 4. This rise time is again interpreted as the formation time of the lowest lying ^{3}MLCT state. The subsequent decay of the excited state is, however, significantly different from that of Ru N3 in solution, as shown by Figure 5b. Since no ground-state bleach recovery was observed (see Figure 5a), the decay of the excited state must produce a new species that is different from the ground state and lowest lying ^{3}MLCT state. We are probing the IR absorption of the lowest lying excited state, not the fluorescence. Therefore, energy transfer between

sensitizers would not cause any decay of the observed signal. One possibility of this intermediate corresponds to the injection of an electron from the dcbpy π^* orbital to the substrate. Although electron injection into the conduction band of Al_2O_3 is not possible in this large band gap material, a pathway involving electron transfer to surface states is possible. Electrons in these surface states in the band gap are far below the conduction band[47] and would not have any significant mid-IR absorption. Since the film is made of nanocrystalline particles, there is a large density of surface states. In a previous experiment with cresyl violet-sensitized Al_2O_3,[36] the fluorescence lifetime of the adsorbed dye at low coverage was found to be shorter compared to those in solution. It was suggested that electron transfer into the surface states in the band gap may be responsible for the observed fluorescence quenching in this large band gap semiconductor.[36] It should be pointed out that large band gap semiconductors such as Al_2O_3 and ZrO_2 have been considered as noninjecting substrates in many previous studies of dye sensitization.[19,22] For $[Ru(bpy)_2(dcbpy)]^{2+}$ adsorbed on Al_2O_3, the overall luminescence decay time was found to be similar to that in solution although there exists a fast decay component in the nanosecond time scale, which was attributed to the excited-state annihilation process between adsorbed dye molecules.[19] The 50% decay of the excited state within 1 ns observed in this experiment suggests that electron injection into surface states in the band gap of these large band gap semiconductor nanomaterials can occur on the sub-nanosecond time scale.

3. Electron Injection from Ru N3 to TiO_2. a. Assignment of the IR Absorption of Injected Electrons. As shown in Figure 6, the observed signal in Ru N3-sensitized TiO_2 films is much larger than Ru N3-sensitized Al_2O_3 films or naked films after 400 nm excitation. For Ru N3-sensitized Al_2O_3, the maximum absorbance change at the peak of the CN stretching band was 4 mOD measured at about 8 μJ pump power as shown in Figure 1b. At the reduced pump power of 1.1 μJ, the amplitude of the signal from the Ru N3 vibrational spectral change can be estimated to be <0.5 mOD, consistent with the lack of transient IR signal for Ru N3-sensitized Al_2O_3, as shown in Figure 6. Therefore, at this low pump power, the changes in the adsorbate vibrational spectrum should not contribute noticeably to the observed signal in Ru N3-sensitized TiO_2 films. The TiO_2 films were prepared with a mixture of anatase and rutile TiO_2 nanoparticles, whose band gaps are 3.2 and 3.0 eV, respectively. The optical absorbance at 400 nm for a typical naked film used in the experiment was about 0.3 OD, with contributions from both absorption to the conduction band in rutile nanoparticles and surface states near the conduction band in anatase nanoparticles as well as scattering of the nanocrystalline films. Excitation of the film at 400 nm can create electrons near the conduction band edge and holes in the valence band[37] leading to the small observed signal (0.6 mOD) shown in Figure 6. Since both Ru N3-sensitized Al_2O_3 and naked TiO_2 films have negligible transient IR signals after 400 nm excitation, the observed 6 mOD signal in the Ru N3-sensitized TiO_2 film cannot be attributed to that of Ru N3 vibrational spectral change or the direct photoexcitation of electron and hole pairs in the naked TiO_2 film. The observed signal must then be due to injected electrons in TiO_2 from the sensitizer. Furthermore, the observed signal is very broad in the mid-IR region. It is present in all the mid-IR wavelengths that we have probed so far ranging from 1700 to 2400 cm^{-1}. This type of broad mid-IR absorption signal can be attributed to injected electrons and has been shown for injected electrons in TiO_2 nanoparticles in colloidal solution[27] and thin films.[8−10] The exact spectral shape of the IR absorption, which can be used to determine the nature of the injected electrons (free vs trapped), is yet to be fully characterized.

b. Electron Injection Time. Since the observed IR absorption shown in Figure 6 is due to injected electrons, its rise time is the electron injection time from the sensitizer to TiO_2. In our earlier Letter,[9] we concentrated on the ultra-fast-injection kinetics and reported a ca. 50 fs injection time. We have since repeated the measurements at many different wavelengths in the 2000−2200 cm^{-1} region. In addition, we have also performed careful measurements in the <100 ps time scale to determine whether there are any multiexponential injection kinetics. As shown in Figures 6−8 as well as listed in Table 1, the best fits to the data in the 2000−2200 cm^{-1} region yield double exponential rise times of 50 ± 25 fs ($>84\%$) and 1.7 ± 0.5 ps ($<16\%$). The ultrafast injection time is still the same as the previously reported value. In addition, we have also observed a small slower rise in the data. We found that this second component was very sensitive to the sample condition. Its amplitude appeared to be bigger in freshly prepared samples and became smaller when the samples aged, although no noticeable difference could be observed from the static UV−vis and FTIR spectra of the films. The exact origin of the second component is so far unknown. More experiments that carefully correlate sample preparation and transient kinetics will be performed to resolve this issue. It is possible that some dye molecules were adsorbed poorly on the surface of TiO_2 in the freshly prepared sample, which may either fall off or eventually bind more strongly, leaving only well-anchored Ru N3 in old samples. Our results clearly demonstrate that $>84\%$ of the electrons are injected in about 50 fs after the excitation of Ru N3 molecules at 400 nm.

It should be pointed out that the instrument response functions used in the deconvolution were determined in a thin silicon wafer, in which 400 nm excitation leads to instantaneous generation of electrons and holes. The Ru N3-sensitized TiO_2 films are highly porous consisting of interconnected nanoparticles of ca. 20 nm average diameter. Although negligible scattering of the probe IR beam is expected, some scattering of the 400 nm pump beam may be possible. This scattering process, if not negligible, may lengthen the effective instrument response function in these porous films compared to those measured in a silicon wafer. We have recently compared the instrument response function (IRF) determined from the rise time of the transient IR signal in a thin silicon wafer and unsensitized TiO_2 thin films, which were prepared under the same condition as those films used for the Ru N3-sensitized samples. It was found that the observed IRF for the porous films was about 20 fs longer than that in the silicon wafer. Since the amount of scattering in the Ru N3-sensitized film may be smaller because of its stronger absorption, the amount of correction for the IRF can be estimated to be <20 fs, although the exact amount of correction needed is unknown. A lengthened instrument response function from scattering would require an even faster rise time to fit the data. Without a more accurate way of measuring the instrument response function in the porous film and the limited time resolution, we cannot exclude the possibility that the electron injection time is even faster than 50 ± 25 fs.

c. Identity of the Injection State. The observed 50 fs injection time from Ru N3 to TiO_2 is on the same time scale or even faster than the intramolecular vibrational energy relaxation as well as intersystem crossing time of adsorbate molecules. The time scale of vibrational energy redistribution for large molecules in solution was often found to be on the order of

10s to 100s of femtoseconds,[38,39] although the exact time scale for Ru N3 has yet to be determined. Electronic relaxation from the initially prepared Franck−Condon state to the long-lived ^{3}MLCT state for $Ru(bpy)_3^{2+}$ in solution was found to occur on the 100 fs time scale.[34] Our measurement of the formation time of the CN stretch mode in the ^{3}MLCT excited state also yields a rise time of <75 fs for Ru N3 in ethanol and adsorbed on Al_2O_3. If we assume a noticeable shift of CN-stretching frequency from ^{1}MLCT state to the ^{3}MLCT state, the measured time suggests that the formation time of ^{3}MLCT state in Ru N3 is also occurring in the <75 fs time scale. While it is possible that electron injection may occur in the same time scale or even prior to vibrational energy redistribution and intersystem crossing, as suggested in a recent paper,[12] our data do not provide unambiguous evidence for the identity of the injection state. Ongoing pump-wavelength-dependent experiments may provide more insight into these important issues. It should be pointed out that in a recent photocurrent measurement on $Fe(dcbpy)_2(CN)_2$-sensitized nanocrystalline TiO_2 film electrodes, evidence for electron injection prior to intersystem crossing from ^{1}MLCT state to lower lying ligand field states was reported.[40]

The exact reason for the ultrafast injection of electron from the sensitizer to TiO_2 is so far unclear. A direct charge-transfer transition from Ru to TiO_2 is not likely in this system because of the lack of spectral overlap between Ru and TiO_2 orbitals. This notion is supported by the observation of only minor red shift of the Ru N3 absorption spectrum when adsorbed on TiO_2.[19] One possibility for the observed fast injection is a strong coupling of the dcbpy π^* orbital with TiO_2, leading to an adiabatic electron transfer from dcbpy to TiO_2. In this case, the optical transition would correspond to excitation from Ru to a mixed state of dcbpy π^* and Ti 3d orbitals, although the initial wave packet is still prepared in the dcbpy side because of Franck−Condon overlap. However, it is still unclear whether strong coupling is necessary for fast interfacial electron-transfer processes from adsorbate to semiconductors, which have large density of states. According to Fermi's golden rule, a large accepting state density in TiO_2 would also give rise to an ultrafast injection time even when the coupling between dcbpy π^* orbital and TiO_2 is weak or intermediate. The extent of electronic coupling and origin of the ultrafast injection dynamics will be investigated in future experiments by systematically varying the coupling strength and density of accepting state.

d. Comparison with Previous Works. Ultrafast electron injection dynamics in Ru N3-sensitized TiO_2 films have been studied by other groups.[12,14] Tachibana et al.[14] reported an almost equal amplitude biphasic-injection process with time constants of <150 fs and 1.2 ps. Here, the electron injection process was identified by measuring the apparent[25,26] transient spectrum in the 500−900 nm region of the oxidized form of Ru N3 dye. The 1.2 ps rise component was directly measured at the peak of the cation absorption at 750 nm. The <150 fs injection component was inferred from the observation that the transient spectrum at 150 fs, the earliest time measured, was already half of the magnitude of the total spectral change at later time. The fast component appears to be consistent with our measured 50 fs injection time. However, the intensity of the second component with 50% of the total amplitude was much bigger than our 1.7 ± 0.5 ps (<16%) component. The origin for the discrepancy is so far unclear. It should be pointed out that the transient visible spectral change measured in the earlier study by Tachibana et al.[14] may contain contributions from vibrational relaxation dynamics of the cation. Ultrafast electron injection may form vibrationally hot cation molecules, whose vibrational cooling time should be on the picosecond time scale. Since >90% of the IR signal observed in our measurement was from injected electrons in TiO_2, the measured kinetics are basically free from the influence of vibrational relaxation dynamics of the sensitizer.

A more recent study of the same system in a UHV chamber[12] reported a different transient absorption in the visible and near-IR regions. The reason for the different transient spectra in UHV and solution is still a subject of further debate.[25,26] In this study a near-IR absorption at 1100 nm was observed and assigned to injected electrons. On the basis of the rise time of the near-IR signal, a <25 fs injection time was obtained. Our measured electron injection time is in agreement with the <25 fs injection time they reported.[12] However, we have recently found that similar near-IR absorptions at 1500 nm could be observed under atmospheric conditions for Ru N3 on TiO_2, N3 in solution, and N3 on ZrO_2 after excitation of the MLCT band.[9] The amplitudes of the latter two signals are about 70% of that for Ru N3-sensitized TiO_2 film under the same pump energy. This result indicates that under atmospheric conditions there may be significant absorption from the sensitizer excited state in the near-IR region.

4. Dynamics of Injected Electrons: Electron Relaxation and Back-Transfer. While the rise of the IR signal indicates the electron injection time from sensitizer to TiO_2, the decay of the IR signal reveals the subsequent dynamics of the injected electrons. The decay of the IR signal can be caused by electron recombination with the oxidized sensitizer and electron relaxation within TiO_2 (electron cooling and trapping). Back electron transfer decreases the population of injected electrons, and relaxation of injected electrons in TiO_2 changes the IR cross section of the electrons. The IR absorption of the injected electrons arises from transitions within states in the conduction band, trap states, or the combination thereof. Since the density of the trap states and states in the conduction band decreases with decreasing energy of the electrons,[37,41] both cooling and trapping of electrons could lead to a decrease of electron IR absorption cross section. Back electron transfer has been shown to occur on the millisecond to microsecond time scale.[14,42] Therefore, the observed decay in the sensitized film can be attributed to electron relaxation dynamics within the TiO_2 film. Electron cooling dynamics are typically <1 ps in bulk semiconductor materials,[43] indicating that the observed slow decay kinetics in Ru N3-sensitized TiO_2 films are probably related to electron trapping. It is interesting to note that the trapping dynamics in the sensitized film are faster than those in a bulk TiO_2 crystal[8,27] but slower than those in colloidal nanoparticles,[8,27,28] consistent with the trend of the density of trap states in these different crystalline TiO_2 materials.

In the unsensitized film, 400 nm excitation leads to generation of electron and hole pairs in TiO_2. In addition to cooling and trapping of electrons, electron hole recombination also leads to the decay of the mid-IR absorption signal. As shown in Figure 9, the mid-IR signal in the naked film decays much faster compared to the sensitized film: at 1 ns, the IR absorption signal decayed by about 50% in the naked film, and by about 15% in the sensitized film. This is also evident in the additional ~10 ps decay component required in fitting the decay kinetics for the naked films. To the best of our knowledge, electron−hole recombination dynamics in TiO_2 nanocrystalline thin films have not been reported previously, although fast electron hole recombination in TiO_2 nanoparticles in solution have been studied.[44−46]

Summary

The photophysics and electron injection dynamics of Ru(dcbpy)$_2$(NCS)$_2$ in solution and adsorbed on Al_2O_3 and TiO_2 thin films have been studied by femtosecond mid-IR spectroscopy. The main experimental results are as follows:

(1) For Ru N3 in ethanol, 400 nm excitation leads to a long-lived excited state with CN stretching bands at 2040 cm^{-1}. This long-lived excited state is assigned to the lowest lying excited state, i.e., the ^{3}MLCT state. The rise time for the transient IR signal for the ^{3}MLCT state was found to be <100 fs. This rise time was tentatively assigned to the formation time of the long-lived ^{3}MLCT state. No decay of the excited absorption at 2040 cm^{-1} was observed within 1 ns, consistent with the previously known 59 ns lifetime.

(2) For Ru N3 absorbed on nanocrystalline Al_2O_3 thin films, a wide band gap semiconductor, a similar shift of CN stretch frequency was observed for the ^{3}MLCT state, which was formed in <75 fs. In contrast to Ru N3 in ethanol, this excited-state decayed by 50% within 1 ns via multiple exponential decay and no ground-state recovery was observed during the same time. This decay is attributed to electron transfer to surface states within the band gap of Al_2O_3.

(3) For Ru N3-sensitized nanocrystalline TiO_2 thin films, the mid-IR signal in the 1700−2400 cm^{-1} region was dominated by injected electrons in TiO_2. The rise time of the mid-IR signal can be fit by biexponential rise functions: 50 ± 25 fs (>84%) and 1.7 ± 0.5 ps (<16%) after deconvolution of instrument response function determined in a thin silicon wafer. Because of the scattering of the pump photons in the porous thin TiO_2 film, the instrument response may be slightly lengthened, which may require a faster rise time for the first component to fit the data. The first component is assigned to electron injection from the Ru N3 excited state to TiO_2. The amplitude of the slower component appeared to change with the sample freshness ranging from ca. 16% in new samples to <5% in aged samples. The origin for this component is so far unclear.

(4) The dynamics of the injected electrons have also been monitored by the decay of the IR signal. The IR signal decays by <20% within 1 ns. This decay is attributed to electron trapping dynamics in TiO_2 films.

This study demonstrates the ability of ultrafast infrared spectroscopy to unambiguously measure interfacial electron transfer rates between molecular sensitizers and semiconductors. The observed fast electron injection time and slow back ET time is consistent with the previously measured almost 100% quantum yield for photon to electron conversion.[6] There remain many questions about the detailed mechanisms of electron injection. The observed electron injection time from the excited state of Ru N3 to TiO_2 appears to be similar to or faster than the typical intramolecular vibrational energy redistribution time and intersystem crossing time in the excited states of Ru N3. A more careful study of the latter two processes may help to establish the relative rates of these processes. A pump wavelength dependence study will also help to address these issues. Furthermore, the properties of the injected electrons are yet to be fully characterized. Ongoing measurements of the time dependent IR spectral evolution in a wider spectral region would provide detailed information about the initial state and subsequent relaxation of the injected electrons.

Acknowledgment. J.B.A., H.N.G., and T.L. of EU thank the financial support by the Petroleum Research Fund, administered by the American Chemical Society, the Emory University Research Committee, and the U.S. Department of Energy. R.J.E., S.F., and A.J.N. were supported by the U.S. Department of Energy, Office of Energy Research, Division of Chemical Sciences.

References and Notes

(1) Miller, R. J. D.; McLendon, G. L.; Nozik, A. J.; Schmickler, W.; Willig, F. In *Surface Electron-Transfer Processes*; VCH Publishers, Inc.: New York, 1995.
(2) Nozik, A. J.; Memming, R. *J. Phys. Chem.* **1996**, *100*, 13061.
(3) Hagfeldt, A.; Gratzel, M. *Chem. Rev.* **1995**, *95*, 49−68.
(4) Kamat, P. V. *Prog. React. Kinet.* **1994**, *19*, 277−316.
(5) Kamat, P. V.; Meisel, D. In *Semiconductor Nanoclusters−Physical, Chemical, and Catalytic Aspects*; Elsevier: Amsterdam, 1997; Vol. 103.
(6) Nazeeruddin, M. K.; Kay, A.; Rodicio, I.; Humphrybaker, R.; Muller, E.; Liska, P.; Vlachopoulos, N.; Gratzel, M. *J. Am. Chem. Soc.* **1993**, *115*, 6382−6390.
(7) Oregan, B.; Gratzel, M. *Nature* **1991**, *353*, 737−740.
(8) Asbury, J. B.; Ghosh, H. N.; Ellingson, R. J.; Ferrere, S.; Nozik, A. J.; Lian, T. Femtosecond IR Study of Ru Dye-Sensitized Nanocrystalline TiO_2 Thin Films: Ultrafast Electron Injection and Relaxation Dynamics, Ultrafast Phenomena XI; Springer-Verlag: Berlin, 1998, in press.
(9) Ellingson, R. J.; Asbury, J. B.; Ferrere, S.; Ghosh, H. N.; Lian, T.; Nozik, A. J. *J. Phys. Chem. B* **1998**, *102*, 6455.
(10) Heimer, T.; Heilweil, E. J. *J. Phys. Chem. B* **1997**, *101*, 10990−10993.
(11) Heimer, T.; Heilweil, E. J. Measuring Ultrafast Sensitizer-TiO2 Electron Dynamics with Mid-Infrared Spectroscopy, Ultrafast Phenomena XI; Springer-Verlag: Berlin, 1998, in press.
(12) Hannappel, T.; Burfeindt, B.; Storck, W.; Willig, F. *J. Phys. Chem. B* **1997**, *101*, 6799−6802.
(13) Eichberger, R.; Willig, F. *Chem. Phys.* **1990**, *141*, 159−173.
(14) Tachibana, Y.; Moser, J. E.; Gratzel, M.; Klug, D. R.; Durrant, J. R. *J. Phys. Chem.* **1996**, *100*, 20056−20062.
(15) Yan, S. G.; Hupp, J. T. *J. Phys. Chem. B* **1997**, *101*, 1493−1495.
(16) Yan, S. G.; Hupp, J. T. *J. Phys. Chem.* **1996**, *100*, 17.
(17) Zaban, A.; Ferrere, S.; Gregg, B. A. *J. Phys. Chem. B* **1998**, *102*, 452.
(18) Zaban, A.; Ferrere, S.; Sprague, J.; Gregg, B. A. *J. Phys. Chem. B* **1997**, *101*, 55.
(19) Vinodgopal, K.; Hua, X.; Dahlgren, R. L.; Lappin, A. G.; Patterson, L. K.; Kamat, P. V. *J. Phys. Chem.* **1995**, *99*, 10883−10889.
(20) Fessenden, R. W.; Kamat, P. V. *J. Phys. Chem.* **1995**, *99*, 12902−12906.
(21) Argazzi, R.; Bignozzi, C. A.; Heimer, T. A.; Castellano, F. N.; Meyer, G. J. *J. Phys. Chem. B* **1997**, *101*, 2591−2597.
(22) Heimer, T. A.; Meyer, G. J. *J. Lumin.* **1996**, *70*, 468−478.
(23) Heimer, T. A.; Darcangelis, S. T.; Farzad, F.; Stipkala, J. M.; Meyer, G. J. *Inorg. Chem.* **1996**, *35*, 5319−5324.
(24) Ford, W. E.; Rodgers, M. A. J. *J. Phys. Chem.* **1994**, *98*, 3822.
(25) Hannappel, T.; Zimmermann, C.; Meissner, B.; Burfeindt, B.; Storck, W.; Willig, F. *J. Phys. Chem. B* **1998**, *102*, 3651.
(26) Moser, J. E.; Noukakis, D.; Bach, U.; Tachibana, Y.; Klug, D.; Durrant, J. R.; Humphry-Baker, R.; Gratzel, M. *J. Phys. Chem. B* **1998**, *102*, 3649.
(27) Ghosh, H. N.; Asbury, J. B.; Lian, T. *J. Phys. Chem. B* **1998**, *102*, 6482−6486.
(28) Ghosh, H. N.; Asbury, J. B.; Weng, Y.; Lian, T. *J. Phys. Chem. B* **1998**, *102*, 10208.
(29) Cavicchia, M. A.; Alfano, R. R. Ultrafast Upper Sattlite Valley Spectroscopic Dynamics using UV pump −IR probe Absorption Spectroscoopy in GaAs and GaP. In *Ultrafast Phenomena in Semiconductors*; Ferry, D. K., van Driel, H. M., Eds.; SPIE: Bellingham, WA, 1994; Vol. 2142; p 128.
(30) Woerner, M.; Elsaesser, T.; Kaiser, W. *Phys. Rev. B* **1992**, *45*, 8378.
(31) Faist, J.; Capasso, F.; Sivco, D. L.; Sirtori, C.; Hutchinson, A. L.; Cho, A. Y. *Science* **1994**, *264*, 553.
(32) Pankove, J. I. In *Optical Processes in Semiconductors*; Dover: New York, 1975.
(33) Lian, T. Q.; Bromberg, S. E.; Asplund, M. C.; Yang, H.; Harris, C. B. *J. Phys. Chem.* **1996**, *100*, 11994−12001.
(34) Damrauer, N. H.; Cerullo, G.; Yeh, A.; Boussie, T. R.; Shank, C. V.; McCusker, J. K. *Science* **1997**, *275*, 54.
(35) Duffy, N.; Dobson, K. D.; Gordon, K. C.; Robinson, B. H. *Chem. Phys. Lett.* **1997**, *266*, 451−455.
(36) Kietzmann, R.; Willig, F.; Weller, H.; Vogel, R.; Nath, D. N.; Eichberger, R.; Liska, P.; Lehnert, J. *Mol. Cryst. Liq. Crys.* **1991**, *194*, 169−180.
(37) Rothenberger, G.; Fitzmaurice, D.; Gratzel, M. *J. Phys. Chem.* **1992**, *96*, 5983.
(38) Mokhtari, A.; Chebira, A.; Chesnoy, J. *J. Opt. Soc. Am. B* **1990**, *7*, 1551.

(39) Laermer, F.; Elsaesser, T. *J. Opt. Soc. Am. B* **1990**, *7*, 1604.
(40) Ferrere, S.; Gregg, B. A. *J. Am. Chem. Soc.* **1998**, *120*, 843.
(41) Kay, A.; Humphrybaker, R.; Gratzel, M. *J. Phys. Chem.* **1994**, *98*, 952−959.
(42) Haque, S. A.; Tachibana, Y.; Klug, D. R.; Durrant, J. R. *J. Phys. Chem. B.* **1998**, *102*.
(43) Shah, J. In *Ultrafast Spectroscopy of Semiconductors and Semiconductor Nanostructures*; Springer-Verlag: Berlin, 1996; Vol. 115.
(44) Colombo, D. P.; Bowman, R. M. *J. Phys. Chem.* **1995**, *99*, 11752−11756.
(45) Skinner, D. E.; Colombo, D. P.; Cavaleri, J. J.; Bowman, R. M. *J. Phys. Chem.* **1995**, *99*, 7853−7856.
(46) Colombo, D. P.; Roussel, K. A.; Saeh, J.; Skinner, D. E.; Cavaleri, J. J.; Bowman, R. M. *Chem. Phys. Lett.* **1995**, *232*, 207−214.
(47) Gautier, M.; Duraud, J. P.; Pham Van, L.; Guittet, M. J. *Surf. Sci.* **1991**, *250*, 71.